DYNAMICS AND HYDRODYNAMIC STABILITY
OF SUBMERGED RIGID TOWED BODIES
OF REVOLUTION

by

S. BASU

A thesis submitted to the Department of
Mechanical Engineering in partial
fulfillment of the requirement of
the degree of Bachelor of Engineering

1972

Vibration and Elastohydrodynamics Res. Lab.
Department of Mechanical Engineering
McGill University
Montreal, Canada

ABSTRACT

A general theory is presented to account for the dynamics of submerged rigid towed bodies. The equations of small lateral motions are derived for the general case of a body of an arbitrary shape as well as for the special cases of cylinder and gradually tapered body of revolution. The criteria of stability are established from the equations of motion.

Some experiments concerning the stability of rigid bodies of revolution under axial flow are described and the theory is tested. The theory is in general qualitative agreement with the experimental observations. No attempt is made presently to draw any definite conclusion on quantitative comparison though quantitative datâ are obtained both from theory and experiments.

ACKNOWLEDGEMENTS

The author is grateful to his research director, Professor M.P. Paidoussis, without whose constant supervision and encouragement the completion of the present work would never have been possible.

The author also gratefully acknowledges the help of Mr. M. Hannoyer throughout the experiments. An acknowledgement is also due to Mr. J. Dubik who undertook the hard task of manufacturing the towed body models.

Lastly, the acknowledgement is made to Miss Pat Lust who has done an excellent job in typing up this thesis.

TABLE OF CONTENTS

CHAPTER 1

INTRODUCTION

In towing operation of an underwater vehicle, the consideration of the dynamic stability of towed vehicle is quite important. Instabilities that may arise in the course of towing operation can be of yawing, pitching or rolling type or can be any combination of these three types. Usually, any form of instability originates from coupled disturbance created by aerodynamic and hydrodynamic forces associated with the towed body. However, the geometric parameters of towed body and of tow-rope may very well affect the stability of the system. In either case, an investigation of the dynamic stability of towed body is of practical importance.

The first substantive study on the subject was made by Strandhagen, Schoenherr and Kobayashi (1) in connection with the towing operation of ships. In their paper, Strandhagen et al. established the criteria for stability of a towed ship and these are: (i) the point of attachment of the tow-rope should be ahead of the center of pressure of both the static lateral hydrodynamic and aerodynamic forces acting on the ships; (ii) the ship should be stable untowed; (iii) if the ship is not stable untowed, then a variation in the length of tow rope should render stability of the ship while towed.

More recently, the stability of submerged towed bodies has been studied by Richardson (2), Patton and Schram (3), Jeffrey (4), Schram and Reyle (5), and by many others. Jeffrey's study indicates the relative significance of the different modes of oscillation and the relative importance of body design and cable configuration effects in each mode. Richardson asserted that the modes of oscillation of a towed body are essentially dependent on the body derivatives and hence on the geometric parameters.

A somewhat different approach to this subject has been motivated by the stability study of the Dracone flexible barge. The analysis of the stability of Dracone barges was first made by Hawthorne (6). Later, the dynamics of flexible slender cylinders in axial flow were studied by Paidoussis (7), (8). He also studied the stability of submerged cylindrical bodies - both flexible and rigid (9), (10). In the case of flexible slender cylinders, stability has been found to be highly dependent on towing speed and both rigid-body type instabilities and flexural instabilities have been shown to exist. That the geometric parameters of the towed body have some effects on the stability were also shown by Paidoussis. It is of great interest, therefore, to study the stability of towed bodies of variable geometric parameters.

In this paper, we shall derive the equations of motion of a submerged rigid towed body of any arbitrary shape. The derivation shall not follow that of Paidoussis. Instead, we shall derive the equations from the classical force and moment balance concept. The total force on the rigid body and the total moment can be obtained by integrating the elemental force and moment fields over the contour of the body. The equations of motions thus obtained will be more general since the shape of the body is fairly arbitrary. As special cases, we shall also derive the equations of motion for a uniform cylindrical rigid body and for a gradually tapered rigid body of revolution. From the equations of motion thus obtained for gradually tapered cylinders, we shall examine the criteria of stability.

CHAPTER 2

EQUATIONS OF SMALL LATERAL MOTIONS IN AXIAL FLOW

We shall derive the equations of small lateral motions of a slender rigid body of revolution, the general shape of which is shown in Figure 1(a). Figure 1(b), (c) and (d) show three particular shapes of a rigid body of revolution, for which cases the stability will be studied later on. The general equation of motion will be presented in the form:

$$M\ddot{q} + C\dot{q} + Kq = 0 \qquad (2.1)$$

where q = generalized co-ordinates

M = generalized inertia element

C = generalized damping element

K = generalized stiffness element

The body is supported by a string (tow-rope) to prevent it from being washed away downstream. It has a mass per unit length of $m(x)$, cross-sectional area $S(x)$, and flexural rigidity $EI(x)$. The fluid is incompressible and has a uniform flow velocity U parallel to the x-axis, which coincides with the longitudinal axis of symmetry of the body in its static equilibrium configuration. It is to be noted that the incompressibility assumption is quite justified since the towed body is to be immersed in axially flowing water.

The general problem of a rigid body in axial flow is extremely complex in nature and in order to achieve any meaningful solution to the problem, certain simplifying assumptions have to be made. The general equations of motion will be derived following these assumptions and hence any subsequent

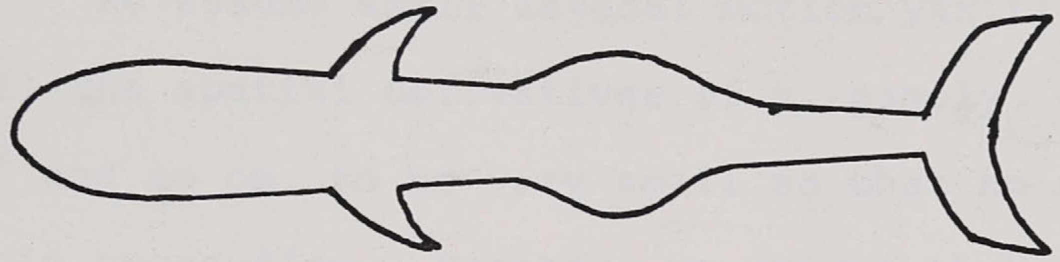

(a) Body of revolution of arbitrary contour

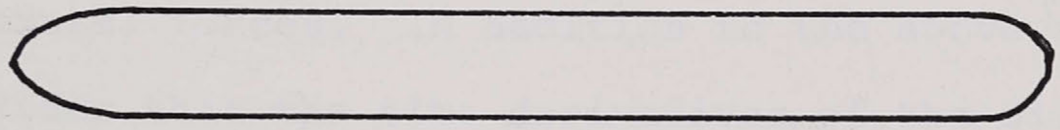

(b) Cylindrical body of revolution

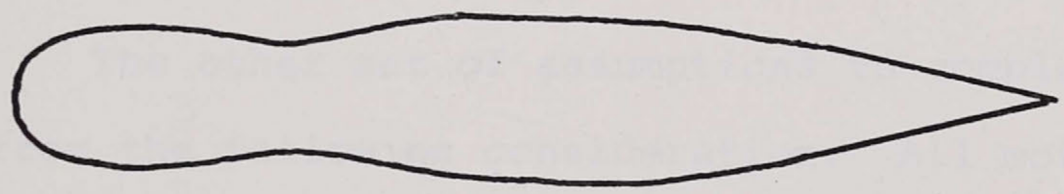

(c) Non-uniform body of revolution with
pointed tail

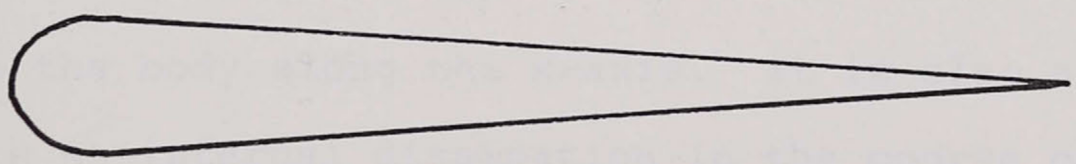

(d) Gradually tapered body of revolution
with pointed tail

Fig. 1 MODELS OF SUBMERGED RIGID TOWED
BODIES

analysis of the problem will be limited by the applicability of the same.

We assume small lateral motion $y(x,t)$ and assume that all the spatial derivatives of y, namely, $\partial y/\partial x$, $\partial^2 y/\partial x^2$ and so on, to be very small so that no separation occurs in cross-flow. Further, we assume that dS/dx and $d(EI)/dx$ are small; the first assumption ensures that no separation occurs in axial flow and the first and second assumptions allow us to use the Euler-beam approximation to describe the flexural forces. In addition to the above assumptions, we consider that the time derivatives of the displacement $y(x,t)$ are small. The last assumption limits the scope of the problem to a great extent and leads to a first order approximation of the actual conditions. For most practical purposes, however, this first order approximation is sufficiently precise.

The other set of assumptions to complete the list comes from the following consideration. All motions are assumed to take place within the (x,y)-plane which is taken to be horizontal. The body is assumed to be neutrally buoyant and to have uniform density. This is to ensure that at zero flow velocity there are no constraining forces or moments in the y-direction to keep the body along the x-axis. It is also assumed that there is no internal dissipation in the course of subsequent motions.

Let us now consider an elemental volume δv of the body. The force and moment systems acting on this elemental volume are shown in Figure 2. F_N and F_L are the normal and longitudinal components of frictional forces per unit length, F_A is the lateral inviscid hydrodynamic force per unit length, F_{BL} is the force per unit length that arises from the boundary layer and sideslip effects, F_T is the boundary forces associated with the elemental volume $\delta v(=\pi r^2(x)\delta x)$. It is to be noted that F_T is a function of T, the axial tension of the tow-rope.

We can now write the force and moment balance equations in the following form:

$$F_x = F_L \cos\theta\,\delta x + (F_N + F_A + F_{BL})\sin\theta\,\delta x - \frac{\partial F_T}{\partial x}\cos\beta\,\delta x \qquad (2.2)$$

$$F_y = -F_L \sin\theta\,\delta x - (F_N + F_A + F_{BL})\cos\theta\,\delta x - \frac{\partial F_T}{\partial x}\cdot\sin\beta\,\delta x - m(x)\frac{\partial^2 y}{\partial t^2}\,\delta x \qquad (2.3)$$

$$M = -F_T\, z(x)\delta x + \left(F_T + \frac{\partial F_T}{\partial x}\right)\left(z(x) + \delta z(x)\right)\delta x \qquad (2.4)$$

where z(x) is the normal distance from the mass center of the elemental volume to the line of action of F_T.

In principle, equations (2.2) to (2.4) can be summed over all the elemental length to obtain the force balance and moment balance equations for the system as a whole. Thus,

$$\sum F_x = \sum F_L \cos\theta\,\delta x - \sum (F_N + F_A + F_{BL})\sin\theta\,\delta x - \sum \frac{\partial F_T}{\partial x}\cos\beta\,\delta x \qquad (2.5)$$

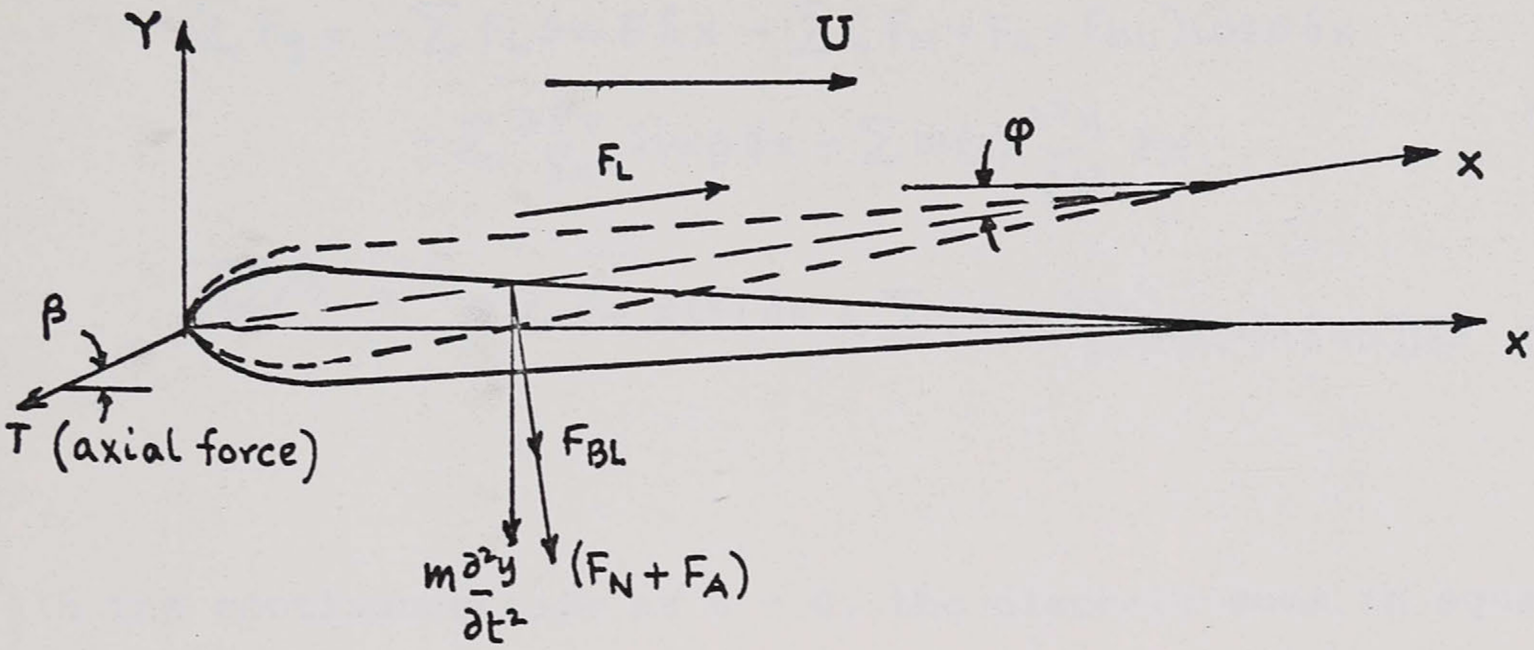

(a) Force and moment systems acting on the ridid body of revolution

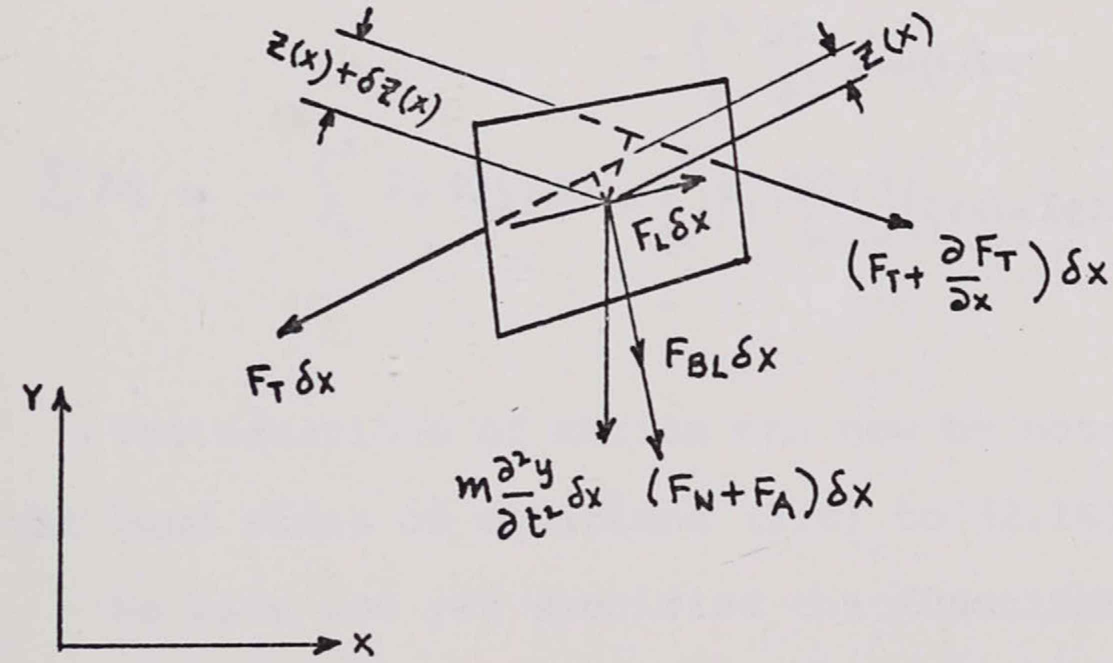

(b) Force and moment systems acting on an element of the body

Fig. 2 DIAGRAM REPRESENTING FORCE AND MOMENT SYSTEMS

$$\sum F_y = -\sum F_L \sin\theta\, \delta x - \sum (F_N + F_A + F_{BL}) \cos\theta\, \delta x$$
$$- \sum \frac{\partial F_T}{\partial x} \sin\beta\, \delta x - \sum m(x) \frac{\partial^2 y}{\partial t^2}\, \delta x \qquad (2.6)$$

$$\sum M = -\sum F_T\, z(x)\, \delta x + \sum \left(F_T + \frac{\partial F_T}{\partial x}\right)\left(z(x) + \delta z(x)\right) \delta x \qquad (2.7)$$

In the continuous case as $\theta \to 0$, the discrete sums in equations (2.5) to (2.7) can be replaced by definite integrals.

$$\sum F_x = \int_0^L F_L\, dx - \int_0^L (F_N + F_A + F_{BL}) \frac{\partial y}{\partial x}\, dx$$
$$- \int_0^L \frac{\partial F_T}{\partial x} \cos\beta\, dx \qquad (2.8)$$

$$\sum F_y = -\int_0^L F_L \frac{\partial y}{\partial x}\, dx - \int_0^L (F_N + F_A + F_{BL})\, dx$$
$$- \int_0^L \frac{\partial F_T}{\partial x} \sin\beta\, dx \qquad (2.9)$$

$$\sum M = -\int_0^L F_T\, z(x)\, dx + \int_0^L \left(F_T + \frac{\partial F_T}{\partial x}\right)\left(z(x) + \delta z(x)\right) dx \qquad (2.10)$$

The equations of motion can now be obtained by equating the right hand sides of equations (2.8) to (2.10) to zero.

We have not yet specified the functional forms of the hydrodynamic forces. Some of these functional forms are expressed as material derivatives of displacement function and hence when they are substituted back into above equations, the integrations becomes very complicated. In order to simplify the situation a little further, we need some added assumptions and these are:

(i) The boundary layer induced force field has little effect in the course of motion of towed body and hence it can be neglected throughout;

(ii) There is no side-slip in the course of motion;

(iii) The integral of boundary forces over the whole length can be equated to the axial force T of the tow-rope.

We now give the functional forms of the hydrodynamic forces. The viscous forces, as proposed by Taylor (11), and elaborated by Paidoussis (7), (8), (12) are given by

$$F_L = \frac{1}{2} C_T \left[\rho S(x)/D(x) \right] U^2 \tag{2.11}$$

$$F_N = \frac{1}{2} C_N \left[\rho S(x)/D(x) \right] U \left[(\partial y/\partial t) + U (\partial y/\partial x) \right] \tag{2.12}$$

where C_T and C_N are the coefficients associated with F_L and F_N respectively, and S(x) and D(x) are the cross-sectional area and the diameter of the body at any distance x.

The axial force, T, at any distance x is given by (12)

$$T(x) = \frac{1}{2} C_2 \rho S(L) U^2 + \frac{1}{2} C_T \rho U^2 \int_x^L \left[S(x)/D(x) \right] dx \tag{2.13}$$

where C_2 is the form-drag coefficient.

The lateral inviscid force, F_A, represents the reaction on the body of the force required to accelerate the fluid around it and, as proposed by Lighthill (13) and later by Paidoussis (12), is given by

$$F_A = \rho S(x) \left[(\partial/\partial t) + U(\partial/\partial x) \right]^2 y + \rho U \left[\left(\frac{\partial y}{\partial t}\right) + U\left(\frac{\partial y}{\partial x}\right) \right] \left(\frac{ds}{dx}\right) \tag{2.14}$$

Let us now substitute the expressions for F_L, F_N, F_A from above to equations (2.8) to (2.10) and carry out the integrations. The equations of motion can thus be obtained as

$$\frac{1}{2}C_T\rho U^2\int_0^L\left[S(x)/D(x)\right]dx - \frac{1}{2}C_N\rho U\int_0^L\left(\frac{S(x)}{D(x)}\right)\left[\left(\frac{\partial y}{\partial t}\right)+U\left(\frac{\partial y}{\partial x}\right)\right]\frac{\partial y}{\partial x}dx$$
$$-\rho\int_0^L S(x)\left[\left(\frac{\partial}{\partial t}\right)+U\left(\frac{\partial}{\partial x}\right)\right]^2 y\,\frac{\partial y}{\partial x}dx - \rho U\int_0^L\left[\left(\frac{\partial y}{\partial t}\right)+U\left(\frac{\partial y}{\partial x}\right)\right] \qquad (2.15)$$
$$\times\left(\frac{ds}{dx}\right)\frac{\partial y}{\partial x}\cdot dx - T\cos\beta = 0$$

$$-\frac{1}{2}C_T\rho U^2\int_0^L\left[S(x)/D(x)\right]\frac{\partial y}{\partial x}dx - \frac{1}{2}C_N\rho U\int_0^L\left(\frac{S(x)}{D(x)}\right)\left[\left(\frac{\partial y}{\partial t}\right)+U\left(\frac{\partial y}{\partial x}\right)\right]dx$$
$$-\rho\int_0^L S(x)\left[\left(\frac{\partial}{\partial t}\right)+U\left(\frac{\partial}{\partial x}\right)\right]^2 y\,dx - \rho U\int_0^L\left[\left(\frac{\partial y}{\partial t}\right)+U\left(\frac{\partial y}{\partial x}\right)\right] \qquad (2.16)$$
$$\times\left(\frac{ds}{dx}\right)\cdot dx - T\sin\beta = 0$$

$$(M)_{TOTAL} = 0 \qquad (2.17)$$

The last of these equations is obtained by assuming that the line of action of the axial force T passes through the mass center of the body about which the moments of all the forces have been taken.

The equations thus derived do not yield any information in that form and to extract anything meaningful, we have to do a non-dimensional analysis of the equations. This means that we have to express these equations in terms of some non-dimensional parameters that have definite physical meaning and hence can be measured experimentally. However, before we step into the non-dimensional analysis in Chapter 4, let us rewrite the integrals of equations (2.15) and (2.16) in neater form. Let us also try to find an explicit form of moment equation (2.17).

Refering to Figure 1(b), let us consider that there are no viscous forces in the small segments of the nose-end and the tail-end of the towed body. Let us also consider that other fluid forces in these segments are multiplied by factors f_1 and f_2 to account for the departures from slender body approximation. Lastly, let us consider that the second order terms are negligible in these small segments. Carrying out the integrations of (2.15) and (2.16) for the nose end of the body over a length ℓ_1, where ℓ_1 is small compared to total body length, L, we get

$$F_1 = (\Sigma F_x)_{nose-end} = -T(0)\cos\beta \tag{2.18}$$

$$\begin{aligned} F_2 = (\Sigma F_y)_{nose-end} &= -f_1 \int_0^{\ell_1} \left\{ \rho s \left[\left(\frac{\partial}{\partial t}\right) + U\left(\frac{\partial}{\partial x}\right)\right]^2 y \right. \\ &\quad \left. + \rho U \left[\left(\frac{\partial y}{\partial t}\right) + U\left(\frac{\partial y}{\partial x}\right)\right]\left(\frac{ds}{dx}\right)\right\} dx - T\sin\beta - \int_0^{\ell_1} m \frac{\partial^2 y}{\partial t^2}\, dx \\ &= -f_1 \rho \frac{\partial^2 y}{\partial t^2} \int_0^{\ell_1} s(x)\,dx - f_1 \rho s U \left(\frac{\partial y}{\partial t} + U\frac{\partial y}{\partial x}\right) \\ &\quad - f_1 \rho U \left(\frac{\partial y}{\partial t} + U\frac{\partial y}{\partial x}\right) \int_0^{\ell_1} \frac{ds}{dx}\,dx - \rho_s \frac{\partial^2 y}{\partial t^2} \int_0^{\ell_1} s(x)\,dx - T\sin\beta \end{aligned}$$

where ρ_s is the density of the material of towed body. Neglecting the $\int_0^{\ell_1} \frac{ds}{dx}\,dx$ term (in comparison to other terms in the expression), we get

$$F_2 = \left[-f_1 \rho S \frac{\partial^2 y}{\partial t^2} x_1 - f_1 \rho S U \left(\frac{\partial y}{\partial t} + U\frac{\partial y}{\partial x}\right) - \rho_s S \frac{\partial^2 y}{\partial t^2} x_1 - T\sin\beta\right]_{x=0}$$

where x_1 is defined by the relation

$$x_1 = \frac{1}{S} \int_0^{\ell_1} s(x)\,dx$$

and S is the cross-sectional area at $x=x_c$, the x-coordinate of the center of gravity of the towed body.

Introducing the virtual mass $M = \rho S$ and $m = \rho_s S$, we finally get

$$F_2 = \left[-x_1 (M f_1 + m) \frac{\partial^2 y}{\partial t^2} - f_1 M U \left(\frac{\partial y}{\partial t} + U\frac{\partial y}{\partial x}\right) - T\sin\beta\right]_{x=0} \tag{2.19}$$

Similarly, carrying the integrations of (2.15) and (2.16) for the tail end of the body over a length ℓ_2 where ℓ_2 is of the same order as ℓ_1 and noting that there is no axial tension at the tail-end, we get,

$$F_3 = (\Sigma F_x)_{\text{tail-end}} = 0 \tag{2.20}$$

$$\begin{aligned} F_4 &= (\Sigma F_y)_{\text{tail-end}} \\ &= -f_2 \int_{L-\ell_2}^{L} \{ \rho s [(\partial/\partial t) + U(\partial/\partial x)]^2 y \\ &\quad + \rho U [\frac{\partial y}{\partial t} + U \frac{\partial y}{\partial x}](\frac{ds}{dx}) \} dx - \int_{L-\ell_2}^{L} m \frac{\partial^2 y}{\partial t^2} dx \\ &= \left[-x_2 (Mf_2 + m) \frac{\partial^2 y}{\partial t^2} + f_2 MU \left(\frac{\partial y}{\partial t} + U \frac{\partial y}{\partial x} \right) \right]_{x=L} , \end{aligned} \tag{2.21}$$

where x_2 is defined by the relation

$$x_2 = \frac{1}{S} \int_{L-\ell_2}^{L} S(x)\, dx$$

We now write the equations of force balance for the main body as

$$\Sigma F_x = F_1 + F_3 - \int_{\ell_1}^{L-\ell_2} F_L\, dx - \int_{\ell_1}^{L-\ell_2} (F_N + F_A) \frac{\partial y}{\partial x} dx = 0 \tag{2.22}$$

$$\begin{aligned} \Sigma F_y = F_2 + F_4 &- \int_{\ell_1}^{L-\ell_2} F_L \frac{\partial y}{\partial x} dx - \int_{\ell_1}^{L-\ell_2} (F_N + F_A)\, dx \\ &- \int_{\ell_1}^{L-\ell_2} m \frac{\partial^2 y}{\partial t^2} dx = 0 \end{aligned} \tag{2.23}$$

For the main body, we shall only be interested in the force balance in y-direction. Following Paidoussis (12), we can approximate equations (2.23) by

$$F_2 + F_4 - \int_0^L F_L \frac{\partial y}{\partial x} dx - \int_0^L (F_N + F_A)\, dx - \int_0^L m \frac{\partial^2 y}{\partial t^2} dx = 0$$

Or,

$$(f_1M+m)x_1\frac{\partial^2 y}{\partial t^2}\Big|_{x=0} + f_1MU\left(\frac{\partial y}{\partial t}+U\frac{\partial y}{\partial x}\right)\Big|_{x=0}$$
$$+ \frac{1}{2}MU^2\left(C_1+C_2+C_T\frac{L}{D}\right)\sin\beta + (f_2M+m)x_2\frac{\partial^2 y}{\partial t^2}\Big|_{x=L}$$
$$- f_2MU\left(\frac{\partial y}{\partial t}+U\frac{\partial y}{\partial x}\right)\Big|_{x=L} + \int_0^L \frac{1}{2}C_T(\rho S/D)\,U^2\frac{\partial y}{\partial x}\,dx$$
$$+\int_0^L\Big\{\frac{1}{2}C_N(\rho S/D)\,U\,[(\partial y/\partial t)+U(\partial y/\partial x)] + \rho S\,[(\partial/\partial t)+U(\partial/\partial x)]^2 y$$
$$+\rho U\left[\left(\frac{\partial y}{\partial t}\right)+U\left(\frac{\partial y}{\partial x}\right)\right]\left(\frac{dS}{dx}\right)\Big\}dx + \int_0^L m(x)\frac{\partial^2 y}{\partial t^2}\,dx = 0 \qquad (2.24)$$

where T is replaced by $\frac{1}{2}MU^2(C_1+C_2+C_T\frac{L}{D})$, C_1 and C_2 being the form drag coefficients and D is the diameter at mass center.

In order to obtain the moment equation, we multiply the force terms in equation (2.16) by x and carryout the integrations in the manner described above. This gives

$$-(f_1M+m)x_3L\frac{\partial^2 y}{\partial t^2}\Big|_{x=0} - f_1MUL\left(\frac{\partial y}{\partial t}+U\frac{\partial y}{\partial x}\right)\Big|_{x=0}$$
$$+\frac{1}{2}MU^2L\left(C_1+C_2+C_T\frac{L}{D}\right)\sin\beta + (f_2M+m)x_4L\frac{\partial^2 y}{\partial t^2}\Big|_{x=L}$$
$$- f_2MUL\left(\frac{\partial y}{\partial t}+U\frac{\partial y}{\partial x}\right)\Big|_{x=L} + \int_0^L\frac{1}{2}C_T(\rho S/D)\,U^2x\frac{\partial y}{\partial x}\,dx$$
$$+\int_0^L\Big\{\frac{1}{2}C_N(\rho S/D)\,U[(\partial y/\partial t)+U(\partial y/\partial x)] + \rho S\,[(\partial/\partial t)+U(\partial/\partial x)]^2y$$
$$+\rho U\left[\left(\frac{\partial y}{\partial t}\right)+U\left(\frac{\partial y}{\partial x}\right)\right]\left(\frac{dS}{dx}\right)\Big\}x\,dx + \int_0^L m(x)\frac{\partial^2 y}{\partial t^2}x\,dx = 0 \qquad (2.25)$$

where

$$x_3 = \frac{1}{SL}\int_0^{\ell_1} x\,S(x)\,dx \quad \text{and} \quad x_4 = \frac{1}{SL}\int_{L-\ell_2}^{L} x\,S(x)\,dx$$

Equations (2.24) and (2.25) represent the equations of motion of a submerged rigid towed body of any arbitrary shape.

CHAPTER 3

EQUATIONS OF MOTIONS FOR SPECIAL CASES

3.1 Cylinder

For a cylinder S is constant and hence dS/dx = 0. Also, due to the symmetry of the body, we can integrate the force and moment terms in (2.24) and (2.25) from -L/2 to L/2 instead of from 0 to L. Then,

$$
\begin{aligned}
&(f_1M+m)x_1\frac{\partial^2 y}{\partial t^2}\Big|_{x=-L/2} + f_1MU\left(\frac{\partial y}{\partial t}+U\frac{\partial y}{\partial x}\right)\Big|_{x=-L/2} \\
&+\frac{1}{2}MU^2C_{TP}\frac{y_N}{s} + (f_2M+m)x_2\frac{\partial^2 y}{\partial t^2}\Big|_{x=L/2} - f_2MU\left(\frac{\partial y}{\partial t}+U\frac{\partial y}{\partial x}\right)\Big|_{x=L/2} \\
&+\int_{-L/2}^{L/2}\frac{1}{2}C_T(\rho S/D)U^2\frac{\partial y}{\partial x}dx + \int_{-L/2}^{L/2}\frac{1}{2}C_N(\rho S/D)U\left[\frac{\partial y}{\partial t}+U\frac{\partial y}{\partial x}\right]dx \\
&+\int_{-L/2}^{L/2}\rho S\left[(\partial/\partial t)+U(\partial/\partial x)\right]^2 y\,dx + \int_{-L/2}^{L/2}m(x)\frac{\partial^2 y}{\partial t^2}dx = 0
\end{aligned}
\tag{3.1}
$$

where $C_{TP} = C_1 + C_2 + C_T\frac{L}{D}$, Y_N is the y-coordinate of the tow point and s is the length of the tow rope. Also,

$$
\begin{aligned}
&-(f_1M+m)x_3L\frac{\partial^2 y}{\partial t^2}\Big|_{x=-L/2} - f_1MUL\left(\frac{\partial y}{\partial t}+U\frac{\partial y}{\partial x}\right)\Big|_{x=-L/2} \\
&+\frac{1}{2}MU^2C_{TP}L\frac{y_N}{s} + (f_2M+m)x_4L\frac{\partial^2 y}{\partial t^2}\Big|_{x=L/2} - f_2MUL\left(\frac{\partial y}{\partial t}+U\frac{\partial y}{\partial x}\right)\Big|_{x=L/2} \\
&+\int_{-L/2}^{L/2}\frac{1}{2}C_T(\rho S/D)U^2x\frac{\partial y}{\partial x}dx + \int_{-L/2}^{L/2}\frac{1}{2}C_N(\rho S/D)U\left[\frac{\partial y}{\partial t}+U\frac{\partial y}{\partial x}\right]x\,dx \\
&+\int_{-L/2}^{L/2}\rho S\left[(\partial/\partial t)+U(\partial/\partial x)\right]^2 y\,x\,dx + \int_{-L/2}^{L/2}m(x)\frac{\partial^2 y}{\partial t^2}x\,dx = 0
\end{aligned}
\tag{3.2}
$$

For rigid-body motion, let us now take the generalized coordinates to be the lateral displacement of the mass center, y_c and the angle that the body makes with the x-axis, ϕ. The displacement at any point will then be given by

$$y(x,t) = y_c(x,t) + x\phi(x,t) \tag{3.3}$$

Substituting equation (3.3) into (3.1) and (3.2), we obtain the equations of motion for a cylindrical body as

$$\begin{aligned}&[M(L+x_1f_1+x_2f_2)+m(L+x_1+x_2)]\ddot{y}_c+[\tfrac{1}{2}C_N\tfrac{MUL}{D}\\&+MU(f_1-f_2)]\dot{y}_c+\tfrac{1}{2s}MU^2C_{TP}\,y_c+\tfrac{L}{2}[M(x_2f_2-x_1f_1)\\&+m(x_2-x_1)]\ddot{\varphi}+MUL\left(2-\tfrac{f_1+f_2}{2}\right)\dot{\varphi}\\&+\left[(f_1-f_2)+\tfrac{1}{2}(C_T+C_N)\tfrac{L}{D}-\tfrac{L}{4s}\right]MU^2\varphi=0\end{aligned} \tag{3.4}$$

and,

$$\begin{aligned}&-\tfrac{1}{2}[ML(x_3f_1-x_4f_2)+mL(x_3-x_4)]\ddot{y}_c-\tfrac{1}{2}MUL(f_1+f_2)\dot{y}_c\\&-\tfrac{L}{4s}MU^2C_{TP}\,y_c+\left[ML^2\left(\tfrac{L}{12}+\tfrac{x_3f_1+x_4f_2}{4}\right)+mL^2\left(\tfrac{L}{12}+\tfrac{x_3+x_4}{4}\right)\right]\ddot{\varphi}\\&+MUL^2\left[\tfrac{f_1-f_2}{2}+\tfrac{1}{24}C_N\tfrac{L}{D}\right]\dot{\varphi}+MU^2L\left[\tfrac{1}{8}\tfrac{L}{s}C_{TP}-\tfrac{f_1+f_2}{2}\right]\varphi=0\end{aligned} \tag{3.5}$$

Similar solutions were obtained by Paidoussis using the theory of (12), namely

$$\begin{aligned}&[M(L+x_1f_1+x_2f_2)+m(L+x_1+x_2)]\ddot{y}_c+[\tfrac{1}{2}C_N\tfrac{MUL}{D}\\&+MU(f_1-f_2)]\dot{y}_c+\tfrac{1}{2s}MU^2C_{TP}\,y_c+\tfrac{L}{2}[M(x_2f_2-x_1f_1)\\&+m(x_2-x_1)]\ddot{\varphi}+MUL\left(2-\tfrac{f_1+f_2}{2}\right)\dot{\varphi}\\&+\left[(f_1-f_2)+\tfrac{1}{2}(C_T+C_N)\tfrac{L}{D}-\tfrac{L}{4s}\right]MU^2\varphi=0\end{aligned} \tag{3.4a}$$

and

$$-\frac{1}{2}\left[ML(x_1f_1-x_2f_2)+mL(x_1-x_2)\right]\ddot{y}_c-\frac{1}{2}MUL(f_1+f_2)\dot{y}_c$$

$$-\frac{L}{4\lambda}MU^2C_{TP}\,y_c+\frac{1}{2}\left[ML^2\left(\frac{L}{12}+\frac{x_1f_1+x_2f_2}{4}\right)+mL^2\left(\frac{L}{12}+\frac{x_1+x_2}{4}\right)\right]\ddot{\varphi}$$

$$+MUL^2\left[\frac{f_1-f_2}{2}+\frac{1}{24}C_N\frac{L}{D}\right]\dot{\varphi}+MU^2L\left[\frac{1}{8}\frac{L}{\lambda}C_{TP}-\frac{f_1+f_2}{2}\right]\varphi=0$$

(3.5a)

3.2 Non-uniform body of revolution with pointed tail

In this case we cannot consider the force and moment systems at the tail end separately. We have to include them in the force and moment systems of the main body. Therefore, any term with f_2 and x_4 will not appear in the equations of motion. Also, unlike the case of cylindrical body, we have to integrate the force and moment terms, in this case, from 0 to L. Equations (2.24) and (2.25) can now be written as

$$x_1(Mf_1+m)\frac{\partial^2 y}{\partial t^2}\Big|_{x=0}+f_1MU\left(\frac{\partial y}{\partial t}+U\frac{\partial y}{\partial x}\right)\Big|_{x=0}$$

$$+\frac{1}{2}MU^2C_{TP}\frac{y_N}{\lambda}+\int_0^L\frac{1}{2}C_T(\rho S/D)U^2\frac{\partial y}{\partial x}dx+\int_0^L\Big\{\frac{1}{2}C_N(\rho S/D)U\left[\frac{\partial y}{\partial t}+U\frac{\partial y}{\partial x}\right]$$

$$+\rho S\left[(\partial/\partial t)+U(\partial/\partial x)\right]^2y+\rho U\left[(\partial y/\partial t)+U(\partial y/\partial x)\right]\left(\frac{dS}{dx}\right)\Big\}dx$$

$$+\int_0^L m(x)\frac{\partial^2 y}{\partial t^2}dx=0 \qquad (3.6)$$

and

$$-x_3L(Mf_1+m)\frac{\partial^2 y}{\partial t^2}\Big|_{x=0}-f_1MUL\left(\frac{\partial y}{\partial t}+U\frac{\partial y}{\partial x}\right)\Big|_{x=0}$$

$$+\frac{1}{2}MU^2C_{TP}L\frac{y_N}{\lambda}+\int_0^L\frac{1}{2}C_T(\rho S/D)U^2x\frac{\partial y}{\partial x}dx$$

$$+\int_0^L\Big\{\frac{1}{2}C_N(\rho S/D)\left[\frac{\partial y}{\partial t}+U\frac{\partial y}{\partial x}\right]+\rho S\left[(\partial/\partial t)+U(\partial/\partial x)\right]^2y$$

$$+\rho U\left[\left(\frac{\partial y}{\partial t}\right)+U\left(\frac{\partial y}{\partial x}\right)\right]\left(\frac{dS}{dx}\right)\Big\}x\,dx+\int_0^L m(x)\frac{\partial^2 y}{\partial t^2}x\,dx=0 \qquad (3.7)$$

For rigid body motions, we take

$$y = y_n - x\phi \tag{3.8}$$

where y_N is the displacement of the nose-end and ϕ is defined by equation (3.3). Substituting equation (3.8) into equations (3.6) and (3.7), we get

$$\begin{aligned}[x_1(Mf_1+m)+x_5(M+m)]\ddot{y}_N + MU\left[f_1+\tfrac{1}{2}C_N\tfrac{x_6}{D}+x_7\right]\dot{y}_N \\ +\frac{1}{2s}MU^2C_{TP}y_N - Lx_8(M+m)\ddot{\varphi} - MUL\left[\tfrac{1}{2}C_N\tfrac{x_9}{D}+2x_8\right. \\ \left.+x_{10}\right]\dot{\varphi} - MU^2\left[f_1+\frac{x_6}{2D}(C_T+C_N)+x_7\right]\varphi = 0\end{aligned} \tag{3.9}$$

and

$$\begin{aligned}-[x_3L(Mf_1+m)-x_8L(M+m)]\ddot{y}_N - MUL\left[f_1-\tfrac{1}{2}C_N\tfrac{x_9}{D}-x_{10}\right]\dot{y}_N \\ +\frac{1}{2s}MU^2LC_{TP}y_N - L^2x_{11}(M+m)\ddot{\varphi} - MUL^2\left[\tfrac{1}{2}C_N\tfrac{x_{12}}{D}\right. \\ \left.+2x_{11}+x_{13}\right]\dot{\varphi} + MU^2L\left[f_1-\frac{x_9}{2D}(C_T+C_N)-x_{10}\right]\varphi = 0\end{aligned} \tag{3.10}$$

where

$$x_5 = \frac{1}{S}\int_0^L S(x)\,dx$$

$$x_6 = \frac{D}{S}\int_0^L \left[\frac{S(x)}{D(x)}\right]dx$$

$$x_7 = \frac{1}{S}\int_0^L \frac{dS}{dx}\,dx$$

$$x_8 = \frac{1}{SL}\int_0^L x\,S(x)\,dx$$

$$x_9 = \frac{D}{SL}\int_0^L \left[\frac{x\,S(x)}{D(x)}\right]dx$$

$$x_{10} = \frac{1}{SL} \int_0^L x \left(\frac{dS}{dx} \right) dx$$

$$x_{11} = \frac{1}{SL^2} \int_0^L x^2 \, S(x) \, dx$$

$$x_{12} = \frac{D}{SL^2} \int_0^L \left[\frac{x^2 S(x)}{D(x)} \right] dx$$

$$x_{13} = \frac{1}{SL^2} \int_0^L x^2 \left(\frac{dS}{dx} \right) dx$$

(3.11)

Equations (3.9) and (3.10) can be regarded as the equations of motion for a non-uniform body of revolution with pointed tail.

3.3 Gradually tapered body of revolution with pointed tail

The equations of motion in this case are exactly the same as in previous cases. One additional simplification can be made, however, due to the fact that S(x) and D(x) are some known functions of x, namely,

$$D(x) = \frac{L-x}{L} D_0$$

and

$$S(x) = \frac{\pi}{4} \frac{D_0^2}{L^2} (L-x)^2 \qquad (3.12)$$

where D_o is the value of D(x) at x = 0.

Substituting equations (3.12) into (3.11), we get

$$x_5 = \frac{\pi D_0^2}{4SL^2} \int_0^L (L-x)^2 dx$$

$$x_6 = \frac{\pi D D_0}{4SL} \int_0^L (L-x) \, dx$$

$$x_7 = \frac{-\pi D_0^2}{4SL^2}\int_0^L (L-x)\,dx = -\frac{D_0}{DL}x_6$$

$$x_8 = \frac{\pi D_0^2}{4SL^3}\int_0^L x(L-x)^2\,dx$$

$$x_9 = \frac{\pi D D_0}{4SL^2}\int_0^L x(L-x)\,dx$$

$$x_{10} = \frac{-\pi D_0^2}{4SL^3}\int_0^L x(L-x)\,dx = \frac{-D_0 x_9}{DL} \qquad (3.13)$$

$$x_{11} = \frac{\pi D_0^2}{4SL^4}\int_0^L x^2(L-x)^2\,dx$$

$$x_{12} = \frac{\pi D D_0}{4SL^3}\int_0^L x^2(L-x)\,dx$$

$$x_{13} = \frac{-\pi D_0^2}{4SL^4}\int_0^L x^2(L-x)\,dx = -\frac{D_0}{DL}x_{12}$$

The equations of motions are now given by (3.4) and (3.10) where x_1, x_2, . . . etc. are given by (3.13).

In matrix form

$$\begin{bmatrix} x_1(Mf_1+m)+x_5(M+m) & -Lx_8(M+m) \\ -x_3(Mf_1+m)L+x_8(M+m)L & -L^2x_{11}(M+m) \end{bmatrix}\begin{pmatrix}\ddot{y}_N \\ \ddot{\varphi}\end{pmatrix}$$

$$\begin{bmatrix} MU(f_1+\frac{1}{2}C_N\frac{x_6}{D}+x_7) & -MUL(\frac{1}{2}C_N\frac{x_9}{D}+2x_8+x_{10}) \\ -MUL(f_1-\frac{1}{2}C_N\frac{x_9}{D}-x_{10}) & -MUL^2(\frac{1}{2}C_N\frac{x_{12}}{D}+2x_{11}+x_{13}) \end{bmatrix}\begin{pmatrix}\dot{y}_N \\ \dot{\varphi}\end{pmatrix}$$

$$\begin{bmatrix} \frac{1}{2s} M U^2 C_{TP} & -MU^2\left(f_1 + \frac{X_6}{2D}(C_T + C_N) + X_7\right) \\ \frac{1}{2s} M U^2 L C_{TP} & MU^2 L\left(f_1 - \frac{X_9}{2D}(C_T + C_N) - X_{10}\right) \end{bmatrix} \begin{pmatrix} y_N \\ \varphi \end{pmatrix} = \begin{pmatrix} 0 \\ 0 \end{pmatrix} \tag{3.14}$$

Comparing with equations (2.1), we can say

$$[M] = \begin{bmatrix} X_1(Mf_1 + m) + X_5(M+m) & -LX_8(M+m) \\ -X_3(Mf_1+m)L + X_8(M+m)L & -L^2 X_{11}(M+m) \end{bmatrix}$$

$$[C] = \begin{bmatrix} MU\left(f_1 + \frac{1}{2}C_N \frac{X_6}{D} + X_7\right) & -MUL\left(\frac{1}{2}C_N \frac{X_9}{D} + 2X_8 + X_{10}\right) \\ -MUL\left(f_1 - \frac{1}{2}C_N \frac{X_9}{D} - X_{10}\right) & -MUL^2\left(\frac{1}{2}C_N \frac{X_{12}}{D} + 2X_{11} + X_{13}\right) \end{bmatrix}$$

$$[K] = \begin{bmatrix} \frac{1}{2s} M U^2 C_{TP} & -MU^2\left(f_1 + \frac{X_6}{2D}(C_T + C_N) + X_7\right) \\ \frac{1}{2s} M U^2 L C_{TP} & MU^2 L\left(f_1 - \frac{X_9}{2D}(C_T + C_N) - X_{10}\right) \end{bmatrix} \tag{3.15}$$

CHAPTER 4

NON-DIMENSIONAL ANALYSIS

We shall now make an attempt to investigate the dynamics and the stability of the towed body system. The derivation of the frequency equation and its subsequent analysis constitute a major part of this investigation.

For the sake of simplicity, from here on, let us only refer to the gradually tapered body of revolution with pointed tail and the corresponding equations of motion. This, by no means, limits the scope of the method of analysis that will be presented below.

Having known [M], [C], and [K] from equations (3.15)′, we can write the equations of motion as

$$[M]\begin{pmatrix}\ddot{y}_N\\ \ddot{\varphi}\end{pmatrix} + [C]\begin{pmatrix}\dot{y}_N\\ \dot{\varphi}\end{pmatrix} + [K]\begin{pmatrix}y_N\\ \varphi\end{pmatrix} = \begin{pmatrix}0\\ 0\end{pmatrix} \tag{4.1}$$

For the homogeneous case without damping term, the eigenvalues of the system is given by the determinantal equation

$$\det\{\mu[U] - [W]\} = 0 \tag{4.2}$$

where μ's are the eigenvalues, [U] is the unit matrix and [W] is the inverse dynamical matrix and is equal to $[M]^{-1}[K]$.

This method of analysis is quite straight-forward for undamped homogeneous systems and even for a damping homogeneous system, provided that the equations of motion can be decoupled. A more appealing method of solving the general problem of (4.1), however, is that of non-dimensional analysis.

Following Paidoussis (12), we define the following non-dimensional quantities:

$$\eta = \frac{y_N}{L}\ ,\ \Lambda = \frac{s}{L}\ ,\ \varepsilon = \frac{L}{D}\ ,\ \tau = \frac{Ut}{L} \text{ and } \chi_r = \frac{x_r}{L} \text{ for}$$

$r = 1, \ldots, 6, 8, 9, 11, 12.$

It is to be noted that χ_7, χ_{10} and χ_{13} are already non-dimensional by definition and hence we can define

$$\chi_s = x_s \text{ for } s = 7, 10 \text{ and } 13$$

Let us now consider the solutions of the form

$$\eta = He^{i\omega\tau} \quad \text{and} \quad \phi = \Phi e^{i\omega\tau} \tag{4.3}$$

where ω is the dimensionless frequency defined as $\omega = \Omega L/U$, Ω being the complex circular frequency of oscillation.

Substituting the non-dimensional parameters in equations (3.9) to (3.11) and noting that the assumption of neutral buoyancy requires m = M, we get

$$\begin{aligned}&[\chi_1(1+f_1) + 2\chi_5]\ddot{\eta} + [f_1 + \tfrac{1}{2}\epsilon C_N \chi_6 + \chi_7]\dot{\eta} + \frac{1}{2\Lambda} C_{TP}\,\eta \\ &- 2\chi_8\ddot{\varphi} - [\tfrac{1}{2}\epsilon C_N \chi_9 + 2\chi_8 + \chi_{10}]\dot{\varphi} \\ &\qquad - [f_1 + \tfrac{\chi_6}{2}\epsilon(C_T + C_N) + \chi_7]\varphi = 0\end{aligned} \tag{4.4}$$

and

$$\begin{aligned}&[2\chi_8 - \chi_3(1+f_1)]\ddot{\eta} - [f_1 - \tfrac{1}{2}\epsilon C_N \chi_9 - \chi_{10}]\dot{\eta} + \frac{1}{2\Lambda} C_{TP}\,\eta \\ &- 2\chi_{11}\ddot{\varphi} - [\tfrac{1}{2}\epsilon C_N \chi_{12} + 2\chi_{11} + \chi_{13}]\dot{\varphi} \\ &\qquad + [f_1 - \tfrac{\chi_9}{2}\epsilon(C_T + C_N) - \chi_{10}]\varphi = 0\end{aligned} \tag{4.5}$$

Substitution of $\eta = He^{i\omega\tau}$ and $\phi = \Phi e^{i\omega\tau}$ now yields

$$H\left[-\omega^2\{\chi_1(1+f_1)+2\chi_5\}+i\omega\{f_1+\tfrac{1}{2}\epsilon c_N\chi_6+\chi_7\}+\tfrac{1}{2\Lambda}c_{TP}\right]$$

$$+\Phi\left[2\omega^2\chi_8-i\omega\{\tfrac{1}{2}\epsilon c_N\chi_9+2\chi_8+\chi_{10}\}\right.$$

$$\left.-\{f_1+\tfrac{1}{2}\epsilon(c_T+c_N)\chi_6+\chi_7\}\right]=0 \tag{4.6}$$

and

$$H\left[-\omega^2\{2\chi_8-\chi_3(1+f_1)\}-i\omega\{f_1-\tfrac{1}{2}\epsilon c_N\chi_9-\chi_{10}\}+\tfrac{1}{2\Lambda}c_{TP}\right]$$

$$+\Phi\left[2\omega^2\chi_{11}-i\omega\{\tfrac{1}{2}\epsilon c_N\chi_{12}+2\chi_{11}+\chi_{13}\}\right.$$

$$\left.+\{f_1-\tfrac{1}{2}\epsilon(c_T+c_N)\chi_9-\chi_{10}\}\right]=0 \tag{4.7}$$

Or, in matrix form

$$\begin{bmatrix} -\omega^2\{\chi_1(1+f_1)+2\chi_5\}+i\omega\{\tfrac{1}{2}\epsilon c_N\chi_6+\chi_7+f_1\}+\tfrac{1}{2\Lambda}c_{TP} \\ \qquad 2\omega^2\chi_8-i\omega\{\tfrac{1}{2}\epsilon c_N\chi_9+2\chi_8+\chi_{10}\}-\{f_1+\tfrac{1}{2}\epsilon(c_T+c_N)\chi_6+\chi_7\} \\ -\omega^2\{2\chi_8-\chi_3(1+f_1)\}-i\omega\{f_1-\tfrac{1}{2}\epsilon c_N\chi_9-\chi_{10}\}+\tfrac{1}{2\Lambda}c_{TP} \\ \qquad 2\omega^2\chi_{11}-i\omega\{\tfrac{1}{2}\epsilon c_N\chi_{12}+2\chi_{11}+\chi_{13}\}-\{f_1-\tfrac{1}{2}\epsilon(c_T+c_N)\chi_9-\chi_{10}\} \end{bmatrix}$$

$$\times\begin{pmatrix} H \\ \Phi \end{pmatrix}=\begin{pmatrix} 0 \\ 0 \end{pmatrix} \tag{4.7a}$$

For non-trivial solutions of H and Φ, the determinant of the coefficient matrix must be zero. This leads to a quartic in ω, namely

$$\alpha_0+\alpha_1\omega+\alpha_2\omega^2+\alpha_3\omega^3+\alpha_4\omega^4=0 \tag{4.8}$$

CHAPTER 5

STABILITY ANALYSIS

The dimensionless complex frequency ω has been computed numerically for different values of system parameters using equation (4.8). Some of these values are shown in Table I.

In the case of a rigid body, the threshold of yawing instability as defined by Paidoussis (12) implies $\omega = 0$. From equation (4.8), then, we get $\alpha_o = 0$. Now

$$\alpha_o = \frac{C_{TP}}{2\Lambda}\left[\left\{f_1 - \tfrac{1}{2}\epsilon(C_T+C_N)\chi_9 - \chi_{10}\right\} + \left\{f_1 + \tfrac{1}{2}\epsilon(C_T+C_N)\chi_6 + \chi_7\right\}\right],$$

$$= \frac{C_{TP}}{2\Lambda}\left\{2f_1 + \tfrac{1}{2}\epsilon(C_T+C_N)(\chi_6-\chi_9) + (\chi_7-\chi_{10})\right\}$$

Hence $\alpha_o = 0$ implies

$$\frac{C_{TP}}{2\Lambda}\{2f_1 + \frac{1}{2}\varepsilon(C_T + C_N)(\chi_6 - \chi_9) + (\chi_7 - \chi_{10})\} = 0 \qquad (5.1)$$

Equation (5.1) shows that the threshold of yawing instability does not depend on Λ; neither does it depend on C_{TP}. This confirms the result found by Paidoussis (12) for a cylindrical body. We can therefore find the critical value of design parameter f_1 as a function of C_T and C_N, namely

$$f_1 = \frac{1}{4}\{2(\chi_{10} - \chi_7) + \varepsilon(C_T + C_N)(\chi_9 - \chi_6)\} \qquad (5.2)$$

The threshold of oscillatory instability can be determined from the solutions of equation (4.8). In general, the

TABLE I

f_1	Rigid body frequencies for $\varepsilon C_T = 2.0$, $\Lambda = 2.00$, $\varepsilon C_N = 0.0$, $C_1 = 1 - f_1$		
	ω_1	ω_2	ω_3
1.0	4.988	-1.563	0.248-0.016i
0.8	4.513	-1.518	0.344+0.002i
0.6	3.961	-1.451	0.408+0.021i
0.4	3.301	-1.346	0.445+0.043i
0.2	2.466	-1.166	0.431+0.076i
0.0	-0.240	-0.690	0.181+0.848i
f_1	Rigid body frequencies for $\varepsilon C_T = 0.2$, $\Lambda = 10.0$, $\varepsilon C_N = 0.0$, $C_1 = 1 - f_1$		
	ω_1	ω_2	ω_3
1.0	4.955	-1.201	0.238-0.180i
0.8	4.466	-1.123	0.283-0.169i
0.6	3.893	-1.024	0.328-0.158i
0.4	3.201	-0.891	0.376-0.134i
0.2	2.304	-0.708	0.436-0.039i
0.0	0.533	-0.460	0.550+0.346i

roots of the equation, ω_j, will be complex. Also, since the system has an infinite number of degrees of freedom, we have an infinite set of frequencies, ω_j. If the imaginary components of the frequencies, $Im(\omega_j)$ are all positive, then the system will be stable. If, on the other hand, $Im(\omega_j) < 0$, then the system will exhibit instability in the j^{th} mode. If the corresponding real component of the frequency, $Re(\omega_j)$ is equal to zero, the system will be unstable in the yawing sense; if $Re(\omega_j)$ is not equal to zero, the system will be unstable in the oscillatory sense. Hence, the threshold of oscillatory instability implies $Im(\omega_j) < 0$ and $Re(\omega_j) \neq 0$.

Some stability diagrams (cf. Fig. 3-5) are constructed using equations (5.1) and (5.2) to show the relative dependence of stability on various system parameters.

Figures 3 and 4 show the thresholds of yawing and oscillatory instabilities as functions of f_1, εC_T and εC_N for a fixed value of Λ. Figure 5, on the other hand, shows the stabilizing effect of Λ for a fixed value of εC_N and for discrete values of εC_T. The general procedure of construction of all these diagrams was as follows: (a) a set of values of f_1, εC_N, εC_T, C_1 and Λ were selected; (b) the complex frequencies, ω, were computed for the set of values in (a); (c) the critical values of f_1, εC_T and Λ that meet the criteria of oscillatory and yawing instabilities are located in f_1-εC_T or f_1-Λ plane.

A close look at the stability diagrams reveals two pronounced phenomena; the first being that the system is always stable in the oscillatory sense for $\varepsilon C_T = 0.0$ and irrespective

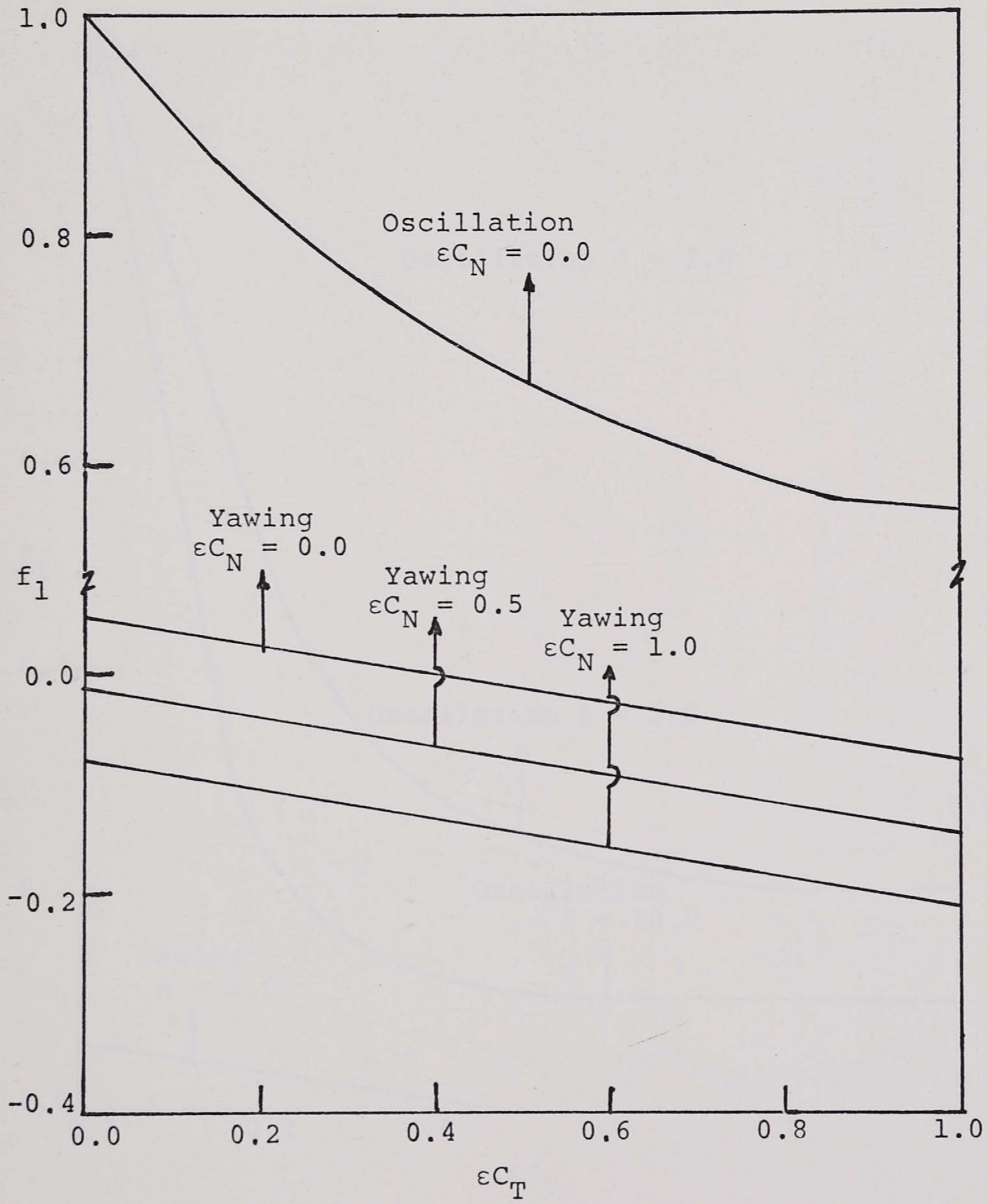

FIGURE 3. The effect of εC_T and f_1 on stability of the rigid body of revolution of FIG. 1(d) with $\Lambda = 2.0$, $C_1 = 1 - f_1$.

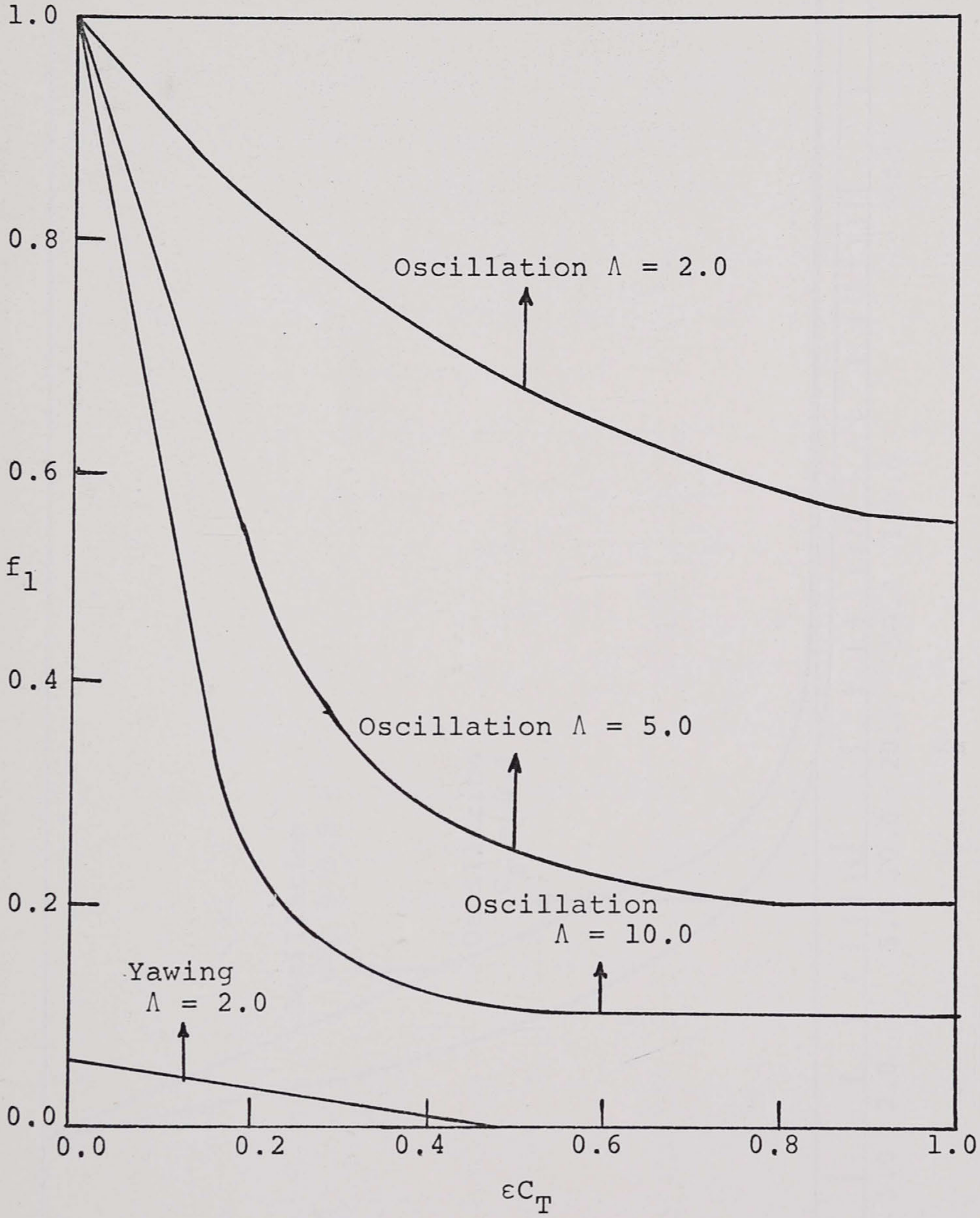

FIGURE 4. The effect of εC_T and f_1 on stability of the rigid body of revolution of FIG. 1(d) with $C_1 = 1 - f_1$ and $\varepsilon C_N = 0.0$

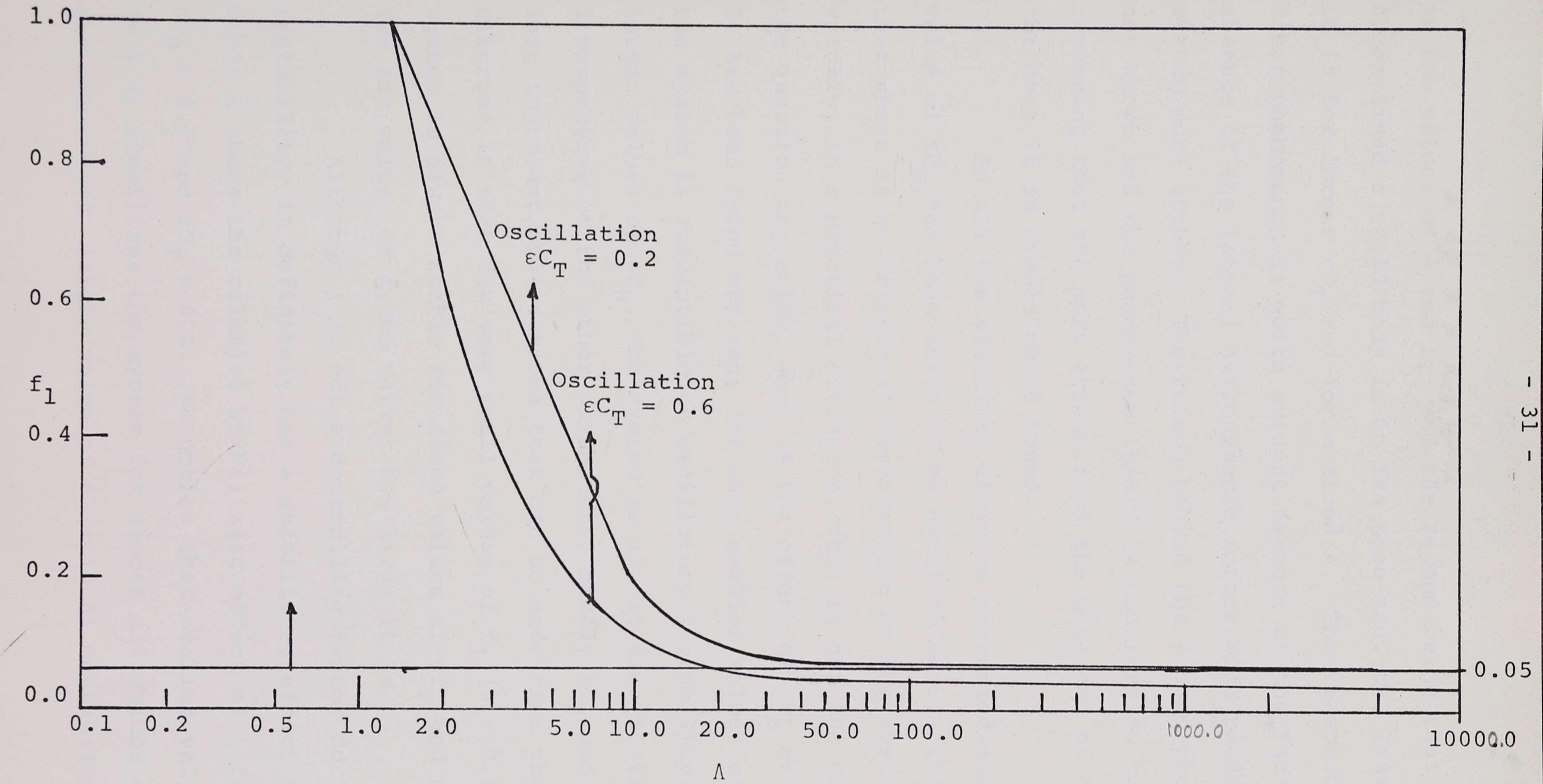

FIGURE 5. The effect of Λ on stability of the rigid body of revolution of FIG. 1(d); $C_1 = 1 - f_1$, $\varepsilon C_N = 0.0$

of the values of Λ and f_1; and the second being that the more streamlined a rigid body is in its nose-end, the less stable it is for larger εC_T and for a fixed Λ. The reason behind the first phenomenon is quite evident because of the fact that the absence of the lateral hydrodynamic forces will render the system more stable. The reason behind the second phenomenon is not known and the phenomenon itself is contrary to the intuitive reasoning that the more streamlined the nose-end of a body is, the more it is stable while towed.

In all the stability diagrams presented above, the value of εC_N has been taken to be equal to zero. This means that there is no frictional force acting on the systems. Obviously, in a practical situation, this is not the case. Hence the question may arise, what is the effect of εC_N on the stability. It has been found out that for only smaller values of εC_N, the system is susceptible to oscillatory instability; for larger values of εC_N, the system is almost always stable irrespective of the other parameters, namely εC_T and f_1. The last important observations that can be made from the stability diagrams is that for very small values of f_1 (0 - 0.03), the system is always stable for fixed values of εC_T and εC_N and for any value of Λ, no matter how large it is.

Although Λ is not a controlling factor for yawing instability, it definitely has a stabilizing effect on the system. Table I shows the relative stabilizing effect of Λ for $\varepsilon C_N = 0.0$ and $\varepsilon C_T = 0.2$. We notice that smaller value of Λ (= 2.0) stabilizes the system for almost all values of f_1; on the other hand, larger value of Λ (= 10.0) destabilizes the system for almost all values of f_1. This is to say that no matter how poorly streamlined the nose-end of a rigid towed body is, a shorter tow-rope will almost always render stability. This can also be apparent from the following consideration.

Let the length of the tow-rope be very large compared to the length of the body. Also, let the form drags of the system be of finite small magnitudes. This means C_{TP}/Λ is very small and in the limiting case $C_{TP}/2\Lambda$ tends to zero. Then for any arbitrary combination of the system parameters f_1, C_N and C_T, the system will exhibit oscillatory instability. On the other hand, systems which are not stable in the oscillatory sense for some values of Λ can be rendered stable for smaller values of Λ.

It is to be noted that the effect of other non-dimensional geometric parameters besides Λ, namely, χ_1, χ_2, . . . , χ_{13} on the stability of the system has not been discussed in this paper. This, by no means, implies that these parameters do not affect the stability. However, within the scope of the present analysis, we have limited ourselves to the stability study of a particular geometry and by doing so any effect of the parameters χ_1, χ_2, . . . χ_{13} on the stability has been eliminated. Incidentally, the values of χ_1, χ_2, . . . χ_{13} have been computed numerically using equations (3.13) and using Simpson's rule of numerical integration. Also, a program has been written to compute the numerical values of the complex frequencies that are roots of the complex polynomial represented by the left hand side of this equation (4.8). The program is shown in the appendix.

CHAPTER 6

EXPERIMENT

6.1 Apparatus

Experiments were conducted with a gradually tapered rigid body of revolution as shown in Fig. 1(d). The body was 8 in. long and 0.5 in. maximum diameter and was made from nylon 6,6 (sp. gr. 1.09-1.14) rod. The nose-end of the body was 7/8 in. long and the contour was parabolic in shape. The sharp pointed tail of the body was produced by a special manufacturing technique. The design criteria of the body were carefully chosen so that the finished body would be neutrally buoyant sectionally. Though the exact result could not be achieved due to manufacturing difficulties, the body was found to be neutrally buoyant as a whole.

The rigid body was held vertically inside an 8 in. diameter glass test-section by a nylon string from a support. The test-section was part of a water tunnel equipped with pump, compressor, exhaust and other accessories. The nylon string could be varied in length. The support was well designed to prevent any separation in axial flow of water. All the tests were carried out under fully developed turbulent pipe flow conditions. All secondary flow effects were eliminated by placing flow-straightening devices before the test-section. The flow velocity was measured with an orifice. The maximum flow velocity attained in this experiment was approximately 5 ft/sec.

6.2 General Observation

Experiments have been carried out for four values of Λ, namely $\Lambda = 1$, 3/4, 1/2 and 1/4. In all cases, at very low flow velocities ($u < 1.87$), the system was stable. At higher flow velocities ($u > 1.87$) yawing instability was observed. In the intermediate flow range ($2.9 \leq u \leq 3.45$), the system started oscillating in addition to yawing. The oscillation was very irregular and it occassionally died down. Mixed modes were suspected to be present in this flow range. Also, the flow range was found to enlarge for different values of Λ. For example, for $\Lambda = 1$, the flow range was $2.9 \leq u \leq 3.24$ whereas for $\Lambda = 1/2$, the flow range was $2.9 \leq u \leq 3.32$. At even higher flow velocities, larger oscillation persisted and predominated over yawing mode. The maximum amplitude of oscillation was found to be increasing with decreasing Λ. For example, at maximum flow velocity ($u = 4.95$), maximum amplitude for $\Lambda = 1$ was 1.4375 in., for $\Lambda = 3/4$, 1.5 in. and for $\Lambda = 1/2$ 1.625 in.

6.3 Results and Discussion

Frequencies have been computed from the experiments for different flow velocities and for different tow-rope lengths. The data are presented in Table II following.

The oscillatory instability was found to persist over a wide range of flow velocities. This is contrary to what had been observed by Paidoussis (12) but in agreement to what had been observed by the same author (7), (8). A possible expla-

TABLE II

Values of Frequency (rad/sec)						
Λ	Flow Velocity u (ft/sec)					
	2.65	3.24	3.75	4.19	4.59	4.95
1	0.795	1.111	1.297	1.448	1.581	1.685
$\frac{3}{4}$	-	1.084	1.336	1.526	1.664	1.783
$\frac{1}{2}$	-	1.043	1.247	1.581	1.782	1.887
$\frac{1}{4}$	-	-	1.275	1.615	1.853	1.989

Other parameters of rigid body:

$$f_1 = 1 - C_1 = 0.8, \ \varepsilon C_N = 1, \ \varepsilon C_T = 1$$

nation of this apparent contradiction can be derived from the fact that in the theory of (<u>12</u>), f_1 has taken to be equal to 1 whereas in the present analysis, f_1 assumes value much closer to 0.8.

CHAPTER 7

CONCLUSION

A general theory has been presented in this paper to account for the dynamics and hydrodynamic stability of submerged rigid towed bodies of any arbitrary shape. The derivation of the theory is different from that of Paidoussis (12); the difference being due to the fact that in the present analysis, the boundary conditions of the dynamic system have been incorporated under the integrals of motion. This renders the present theory more general and the theory of (12) can be considered as a special case of the present theory.

The dynamics and the stability of a gradually tapered body of revolution have been formulated as another special case of the new theory. Only two types of instabilities were found to be present as predicted by the theory and supported by the experimental evidences. These were yawing instability and the first mode oscillatory instability. No attempt has been made, however, to draw any definite conclusions regarding the quantitative comparison between theory and experiment.

Perhaps, the most important feature of the new theory is that it confirms the fact that the length of the tow rope does have no effect on the yawing instability of the towed body; a conclusion that has been reached by Paidoussis (12). The theory also suggests that the absolute threshold of yawing instability does not depend even on C_{TP}. This is again in good agreement to that of (12). The relative stabilizing effect of Λ as predicted by the theory was supported by the experimental observations.

It has been shown in Chapter 5 that the streamlining of the nose-end of the towed body has a pronounced effect on the stability. In fact, contrary to the theory of (12), streamlining of the nose-end makes the body less stable. To justify the above statement, we consider the work done, ΔW, on the rigid body over one period of oscillation, t_1, in much the same way as was done in (8). Thus

$$\Delta W = (1-f_1)MU\int_0^{t_1}\left[\dot{y}^2 + U\dot{y}y'\right]_{x=0}dt - \frac{1}{2}C_N\int_0^{t_1}\int_0^L\left(\frac{MU}{D}\right)\left[\dot{y}^2 + U\dot{y}y'\right]dx\,dt \qquad (7.1)$$

The oscillation will be damped if $\Delta W < 0$ and it will be amplified or, the system will be unstable if $\Delta W > 0$. Now, for arbitrary small U, equation (7.1) can be written as

$$\Delta W = (1-f_1)MU\int_0^{t_1}\dot{y}_N^2\,dt - \frac{1}{2}C_N\int_0^{t_1}\int_0^L\frac{MU}{D}\dot{y}^2\,dx\,dt \qquad (7.2)$$

where $\dot{y}_N$ is the value of $\dot{y}$ at $x = 0$. We note that if there is no viscous force, then a well streamlined nose ($f_1 \sim 1$) can at the best make $\Delta W = 0$. This means only a marginal stability can be achieved. If, on the other hand, the viscous forces are present, then a perfectly streamlined nose-end ($f_1 = 1$) will render stability to the body. Accordingly, we must conclude that well streamlining of the nose-end reduces the normal component of the viscous force drastically. This conclusion also supports why the oscillatory instabilities are indicated by smaller values of εC_N, namely $0 \le \varepsilon C_N \le 0.2$.

We next consider if the above conclusion contradicts the other phenomenon cited in Chapter 5, namely, that for very small values of f_1, the system is always stable for fixed values of εC_T and εC_N and for any value of Λ, no matter how large it is. We note that if $f_1 < 1.0$, the first term of (7.2) is positive. We ask ourselves what happens to the second term. If we do the order of magnitude analysis of both terms in (7.2), we find that the second term is about twice as large in magnitude as the first term for very small f_1 and for relatively small εC_N. This implies $\Delta W < 0$ and hence the system is stable.

The question still remains of how closely the theory can predict the dynamical behaviours of the system that are evidenced by the experiment. Contrary to the prediction of the theory that there is no oscillatory instability for $\Lambda \leq 1$, it has been found experimentally that the oscillatory instability exists for $\Lambda \leq 1$. We therefore seek to explain this contradiction.

We consider the fluid stream as an infinite source of energy. Therefore, if the fluid forces, F_L, F_A and F_N are very large, the energy gained by the towed body from the surrounding fluid will not balance the energy released by the towed body to the fluid. This will result in a non-equilibrium situation leading to an increasingly divergent motion, previously referred to as the yawing motion, of the towed body. This yawing motion manifests itself through the translation and rotation of the body about its static equilibrium position. Ideally, then, this type of divergent motion could give rise to a large angular displacement causing an amplified yawing instability. However, the mechanism of yawing instability is much more complex. The complexity may arise from any form of non-linearity that may be inherent in the nature of fluid forces or it may arise from the non-conservative nature of the system at the free-end of the towed body. In either case, a disturbance is associated with the pure yawing motion. Accordingly, we must conclude that a pure yawing instability can hardly be observed in the course of motion. The conclusion may be supported by the experimental evidence that mixed modes are present in the intermediate flow range. Let us now consider the various hydrodynamic forces acting on the, body when $\phi (= - \partial y/\partial x)$ is large. At this configuration, we consider the work done on the body by the surrounding fluid. Since there is a disturbance associated with the yawing motion the work done will be slightly different from that given by equation (7.2). We, therefore, say that at some angle $\phi = \phi_{max}$ the work done on the body by the fluid forces will be balanced by the work done on the body by the disturbance. Hence the kinetic energy imparted to the body at $\phi = \phi_{max}$ will be zero. This will result in an oscillatory motion. In all, then, we conclude that yawing instability manifests itself through the rotational and translational motion of the body; but a pure yawing type instability can hardly be observed in the course of motion.

The present theory can be extended to take into consideration any other form of hydrodynamic forces that may be acting on the body. Also, the theory, presented in its generalized form can be extended to account for non-linear oscillation. These extensions, while fairly simple conceptually, are mathematically tedious.

The investigation is, by no means, complete lacking mainly on the experimental side. Areas of more practical and of general interest that are yet to be covered are the following. What is the optimum shape of a submerged rigid towed body that can be operated stable over a reasonable speed limit? What are the most significant parameters to render the maximum stability to a towed body? Incidentally, these questions can be answered by the general theory that has just been presented.

REFERENCES

(1) A.G. STRANDHAGEN, K.E. SCHOENHERR, F.M. KOBAYASHI 1950 'The Dynamic Stability on Course of Towed Ships', Trans. Soc. Naval Arch. and Marine Eng., 58, 32-66.

(2) J.R. RICHARDSON 1965 'The Dynamics of Towed Underwater Systems', Eng. Res. Associates Rept. No. 56-1, Toronto, Canada.

(3) K.T. PATTON, J.W. SCHRAM 1966 'Equations of Motion of a Towed Body Moving in a Vertical Plane', Rept. No. 736, U.S. Navy Underwater Sound Lab., Fort Turnbull, Connecticut, U.S.A.

(4) N.E. JEFFREY 1968 'Influence of Design Features on Underwater Towed System Stability', J. of Hydronautics, 2, 205-13.

(5) J.W. SCHRAM, S.P. REYLE 1968 'A Three-Dimensional Dynamic Analysis of a Towed System', J. of Hydronautics, 2, 213-20.

(6) W.R. HAWTHORNE 1961 'The Early Development of the Dracone Flexible Barge', Proc. Inst. Mech. Engrs., 175, 52-83.

(7) M.P. PAIDOUSSIS 1966 'Dynamics of Flexible Slender Cylinders in Axial Flow - Part 1, Theory', J. Fluid Mech., 26, 717-36.

(8) M.P. PAIDOUSSIS 1966 'Dynamics of Flexible Slender Cylinders in Axial Flow - Part 2, Experiments', J. Fluid Mech., 26, 737-51.

(9) M.P. PAIDOUSSIS 1968 'Stability of Towed, Totally Submerged Flexible Cylinders', J. Fluid Mech., 34, 273-97.

(10) M.P. PAIDOUSSIS 1967 'Stability of Towed, Totally Submerged Flexible Cylinders', Rept. Eng. R-5, Atomic Energy of Canada, Chalk River, Ontario, Canada.

(11) G.I. TAYLOR 1952 'Analysis of the Swimming of Long and Narrow Animals', Proc. Roy. Soc. (A), 214, 158-213.

(12) M.P. PAIDOUSSIS 1970 'Dynamics of Submerged Towed Cylinders', M.E.R.L. Technical Note 70-4, Eighth Symposium on Naval Hydrodynamics, Caltech, Pasadena, California, U.S.A.

(13) M.J. LIGHTHILL 1960 'Mathematics and Aeronautics', J. Roy. Aero. Soc., 64, 375-94.

APPENDIX

```
      IMPLICIT COMPLEX*16(C),REAL*8(A,B,D-H,O-Z)
      COMMON AL,ACN,ACT,A1,F1,X1,X3,X5,X6,X7,X8,X9,X10,X11,X12,X13
      COMMON /STORE/C(2,2)
      DIMENSION CRT(4),ANGLE(4),CR(4)
      ACN=0.D0
      ACT=-0.2D0
      DO 1002 JZ=1,6
      ACT=ACT+0.2D0
      N=25
      CI=(0.D0,1.D0)
      AL=0.D0
      DO 333 IX=1,10
      AL=AL+1.D0
      F1=-0.05D0
      DO 333 JX=1,21
      F1=F1+0.05D0
      A1=1.D0-F1
      X1=0.15D0
      X3=0.098D0
      X5=0.75D0
      X6=0.771D0
      X7=-0.1652D0
      X8=0.1882D0
      X9=0.2532D0
      X10=-0.0543D0
      X11=0.075D0
      X12=0.1254D0
      X13=-0.0268D0
      II=1
      KOUNT=0
      DO 2 I=1,4
      CROT=(1.D0,0.D0)
      CTRIL1=(1.D0,5.D0)
      CTRIL2=CTRIL1+(.0001D0,.001D0)
    9 COM =CTRIL1*(CROT**II)
      COM1=(CROT**II)*CTRIL2
      ITER=0
      CA=CDET(COM)
      CB=CDET(COM1)
    4 CX=COM
      ITER=ITER+1
      IF(ITER.GT.N) II=II+1
      CROT=(0.5D0,0.75D0)
      IF(II.EQ.10) GO TO 5
      IF(ITER.GT.N) GO TO 9
      CROT=(1.D0,0.D0)
      COM=COM1-CB*(COM-COM1)/(CA-CB)
      COM1=CX
      CB=CA
      CA=CDET(COM)
      A=CA
      B=CB*CI
      Z=DSQRT(A*A+B*B)
      IF(KOUNT.EQ.0) GO TO 6
```

```
      DO 3 K=1,KOUNT
    3 CA=CA/(COM-CRT(K))
    6 CONTINUE
      IF(Z.LE.1.D-08) GO TO 10
      GO TO 4
   10 KOUNT=KOUNT+1
      CC=C(1,2)/C(1,1)
      AA=CI*CC
      BB=-(.5D0,0.D0)-CC
      AA=AA/BB
      ANGLE(KOUNT)=180.D0*DATAN(AA)/3.141592
      CRT(I)=COM
      CR(I)=-CC-(.5D0,0.D0)
      IF(KOUNT.EQ.4) GO TO 5
    2 CONTINUE
    5 WRITE(6,100)CRT,F1,AL
  100 FORMAT(2(/4D22.10),2F15.2)
      CTRIL1=COM
      CTRIL2=CTRIL1+(.0001D0,.001D0)
      WRITE(6,102)ANGLE,ACN,ACT
  102 FORMAT(/5X'PHASE DIFFERENCE =  ',4F10.2,'  DEGREES   ACN =  ',F10.
     12,'  ACT = ',F10.2)
      WRITE(6,103)A1
  103 FORMAT(5X,'  A1 = ',F10.2)
      WRITE(6,356)CR
  356 FORMAT(8F12.3)
      II=1
    1 CONTINUE
  333 CONTINUE
      WRITE(6,2001)
 2001 FORMAT(1H1)
 1001 CONTINUE
 1002  CONTINUE
      STOP
      END
```

```
      COMPLEX FUNCTION CDET*16(COM)
      IMPLICIT COMPLEX*16(C),REAL*8(A,B,D-H,O-Z)
      COMMON AL,ACN,ACT,A1,F1,X1,X3,X5,X6,X7,X8,X9,X10,X11,X12,X13
      COMMON /STORE/C(2,2)
      CI=(0.D0,1.D0)
      XA=X1*(1.0D0+F1)+2.D0*X5
      XB=F1+0.5D0*ACN*X6+X7
      XC=(A1+ACT)/(2.D0*AL)
      XD=-2.D0*X8
      XE=-X10-2.D0*X8-0.5D0*ACN*X9
      XF=-X7-F1-0.5D0*X6*(ACT+ACN)
      C(1,1)=CI*COM*(XA*CI*COM+XB)+XC
      C(1,2)=CI*COM*(XD*CI*COM+XE)+XF
      XA=2.D0*X8-X3*(1.D0+F1)
      XB=X10+0.5D0*ACN*X9-F1
      XC=(A1+ACT)/(2.D0*AL)
      XD=-2.D0*X11
      XE=-X13-2.D0*X11-0.5D0*ACN*X12
      XF=F1-X10-0.5D0*X9*(ACN+ACT)
      C(2,1)=CI*COM*(XA*CI*COM+XB)+XC
      C(2,2)=CI*COM*(XD*CI*COM+XE)+XF
      CDET=C(1,1)*C(2,2)-C(1,2)*C(2,1)
      RETURN
      END
```